Dynamic Screening for ℓ_2-norm Penalized Unbalanced Optimal Transport Problem

Anonymous Author
Anonymous Institution

Abstract

HK comment: We change the story: (OT and UOT $\rightarrow$ Lasso-type UOT $\rightarrow$ Propose Screening (No literature) $\rightarrow$ Evaluation) The Safe Screening technique saves computational time by freezing the zero elements in the sparse solution of the Lasso problem. Recently, researchers have linked the UOT problem to the Lasso problem. In this paper, we apply the newest Dynamic Screening framework to the ℓ_2-norm penalized Unbalanced Optimal Transport (UOT) problem. We first apply the Screening method to the UOT problem. We find out that the specific structure for the UOT problem allows it to get better screening results than the Lasso problem. We propose the new Dynamic Screening algorithm and demonstrate its extraordinary effectiveness and potential to benefit from the unique structure of the UOT problem, our algorithm substantially improves the screening efficiency compared to the standard Lasso Screening algorithm without significantly increasing the computational burden. We demonstrate the advantages of the algorithm through some experiments on the Gaussian distributions and the MNIST dataset.

1 INTRODUCTION

Optimal transport (OT) has a long history in mathematics and has recently become prevalent due to its extraordinary performances in machine learning and statistical learning fields for measuring distances between two probability measures. It has outperformed traditional methods in many different areas such as domain adaptation (Courty, 2017), generative models (Arjovsky et al., 2017), graph machine learning (Maretic et al., 2019) and natural language processing (Chen et al., 2019). The popularity of OT is attributed to the introduction of the Sinkhorn's algorithm (Sinkhorn, 1974) for the entropy-regularized Kantorovich formulation problem (Cuturi, 2013), which alleviates the computational burden in large-scale problems.

Addressing one limitation that the standard OT problem handles only *balanced* samples, the unbalanced optimal transport (UOT) has been proposed envisioning a wider range of applications with *unbalanced* samples (Caffarelli and McCann, 2010; Chizat et al., 2017). This application fields include, for example, computational biology (Schiebinger et al., 2019), machine learning (Janati et al., 2019) and deep learning (Yang and Uhler, 2019). Mathematically, UOT replaces the equality constraints with penalty functions on the marginal distributions with a divergence including KL divergence (Liero et al., 2018), and ℓ_1-norm (Caffarelli and McCann, 2010) and ℓ_2-norm distances (Benamou, Jean-David, 2003). The KL-penalized UOT with an entropy regularizer can be solved by the Sinkhorn algorithm (Pham et al., 2020). It is fast, scalable, and differentiable, but suffers from a larger error of KL divergence, instability (Schmitzer, 2016), and a lack of sparsity in solution compared with other regularizers (Blondel et al., 2018). In contrast, ℓ_2-norm regularized UOT not only indicates a lower error, but also brings a sparse solution. This attracted the attention of researchers, and many algorithms have been developed (Blondel et al., 2018; Nguyen et al., 2022).

Despite of the success in the development of fast and efficient optimization algorithms for UOT, computational burden still remains as a bottleneck for the large-scale application. This paper tackles this issue from a different direction independent of optimization algorithms. Recently, Chapel et al. (2021) suggested a mutual connection between the UOT problem and the Lasso-like problem (Tibshirani, 1996; Efron et al., 2004) and the non-negative matrix factorization prob-

lem (Lee and Seung, 2000). This motivates us to adapt *safe screening* (Ghaoui et al., 2010) in these fields to accelerate the computation of the UOT problem. In fact, the OT and UOT problems expect the solution to be sparse due to the effectiveness of their optimal transport cost, and thus shares the similar idea with the Lasso problem. Safe screening in the Lasso problem is a promising technique to speed up the computation by exploiting the sparsity of the solution. It eliminates elements in the solution that are guaranteed to be zero without solving the optimization problem. However, this straightforward application is not trivial, and the standard Lasso screening method cannot be applied directly to the UOT problem because it has un-regularized elements (what means?). Specifically, while the Lasso problem has a dense *constraint matrix*, that of the UOT problem is extremely sparse and has a unique transport matrix structure. This would benefit a design of specialized screening method and the outcome.

In this paper, we propose a new dynamic screening method designated to the UOT problem. To this end, we first derive a dual formulation of the vectorized Lasso-like UOT problem. Then, particularly addressing the structure of the constraint matrix, a dynamic screening method is derived, which includes a new projection method and a screening region construction method. These are suitable for the UOT problem and could largely improve the effects. Different from the screening method in the Lasso problem, our proposed methods are ....

Contributions.:

- To the best of our knowledge, this work is a first dynamic screening method designated to the UOT problem, which is based on the Lasso-like formulation of the UOT problem and its dual formulation. Our proposed method is independent of optimization algorithms.

- We propose a projection method by leveraging the specific structure of the UOT problem, and it largely decreases the errors in the projection process. We also propose a flexible two hyperplane method for every primal element to construct screening regions.

- Numerical evaluation reveals their effectiveness in terms of projection distances and screening ratios comparing several methods including state-of-the-art methods in the Lasso problem.

The paper is organized as follows. **Section 2** presents preliminary descriptions of optimal transport and unbalanced optimal transport. The screening methods in Lasso-like problems are explained by addressing a dynamic screening framework. In **Section 3**, our proposed screening method for the UOT problem is detailed. **Section 4** shows numerical experiments.

2 PRELIMINARIES

$\mathbb{R}^n$ denotes n-dimensional Euclidean space, and $\mathbb{R}^n_+$ denotes the set of vectors in which all elements are non-negative. $\mathbb{R}^{m \times n}$ represents the set of $m \times n$ matrices. Also, $\mathbb{R}^{m \times n}_+$ stands for the set of $m \times n$ matrices in which all elements are non-negative. We present vectors as bold lower-case letters $\boldsymbol{a}, \boldsymbol{b}, \boldsymbol{c}, \ldots$ and matrices as bold-face upper-case letters $\mathbf{A}, \mathbf{B}, \mathbf{C}, \ldots$. The i-th element of $\boldsymbol{a}$ and the element at the (i, j) position of $\mathbf{A}$ are represented respectively as a_i and $\mathbf{A}_{i,j}$. In addition, $\mathbb{1}_n \in \mathbb{R}^n$ is the n-dimensional vector in which all the elements are one. For $\boldsymbol{x}$ and $\boldsymbol{y}$ of the same size, $\langle \boldsymbol{x}, \boldsymbol{y} \rangle = \boldsymbol{x}^T \boldsymbol{y}$ is the Euclidean dot-product between vectors. For two matrices of the same size $\mathbf{A}$ and $\mathbf{B}$, $\langle \mathbf{A}, \mathbf{B} \rangle = \text{tr}(\mathbf{A}^T \mathbf{B})$ is the Frobenius dot-product. We use $\|\boldsymbol{a}\|_2$ and $\|\boldsymbol{a}\|_1$ to represent the ℓ_2 norm and ℓ_1 norm of $\boldsymbol{a}$, respectively. D_ϕ is the Bregman divergence with the strictly convex and differentiable function ϕ, i.e., $D_\phi(\boldsymbol{a}, \boldsymbol{b}) = \sum_i d_\phi(a_i, b_i) = \sum_i [\phi(a_i) - \phi(b_i) - \phi'(b_i)(a_i - b_i)]$. In addition, we suggests a vectorization for $\mathbf{A} \in \mathbb{R}^{m \times n}$ as a lowercase letters $\boldsymbol{a} \in \mathbb{R}^{mn}$ and $\boldsymbol{a} = \text{vec}(\mathbf{A}) = [\mathbf{A}_{1,1}, \mathbf{A}_{1,2}, \cdots, \mathbf{A}_{m,n-1}, \mathbf{A}_{m,n}]$.

2.1 Optimal Transport and Unbalanced Optimal Transport

Optimal Transport (OT): Given two discrete probability measures $\boldsymbol{a} \in \mathbb{R}^m$ and $\boldsymbol{b} \in \mathbb{R}^n$, the standard OT problem seeks a corresponding *transport matrix* $\mathbf{T} \in \mathbb{R}^{m \times n}_+$ that minimizes the total transport cost (Kantorovich, 1942). This is a linear programming problem formulated as

$$\text{OT}(\boldsymbol{a}, \boldsymbol{b}) \quad := \quad \min_{\mathbf{T} \in \mathbb{R}^{m \times n}_+} \langle \mathbf{C}, \mathbf{T} \rangle \qquad (1)$$

$$\text{subject to} \qquad \mathbf{T} \mathbb{1}_n = \boldsymbol{a}, \mathbf{T}^T \mathbb{1}_m = \boldsymbol{b},$$

where $\mathbf{C} \in \mathbb{R}_+^{m \times n}$ is the *cost matrix*. The constraints in (1) are so-called *mass-conservation constraints* or *marginal constraints*, and assume $\|\boldsymbol{a}\|_1 = \|\boldsymbol{b}\|_1$. Thus, the solution $\hat{\boldsymbol{t}}$ does not exist when $\|\boldsymbol{a}\|_1 \neq \|\boldsymbol{b}\|_1$. The obtained OT matrix $\mathbf{T}^*$ brings powerful distances as $\mathcal{W}_p = \langle \mathbf{T}^*, \mathbf{C} \rangle^{\frac{1}{p}}$, which is known as the p-th order *Wasserstein distance* (Villani, 2008).

As $\boldsymbol{t} = \text{vec}(\mathbf{T}) \in \mathbb{R}^{mn}$ and $\boldsymbol{c} = \text{vec}(\mathbf{C}) \in \mathbb{R}^{mn}$, we reformulate Eq.(1) in a vector format as (Chapel et al.,

2021)

$$\text{OT}(\boldsymbol{a}, \boldsymbol{b}) \quad := \quad \min_{\boldsymbol{t} \in \mathbb{R}_+^{mn}} \boldsymbol{c}^T \boldsymbol{t} \qquad (2)$$

$$\text{subject to} \qquad \mathbf{N}\boldsymbol{t} = \boldsymbol{a}, \mathbf{M}\boldsymbol{t} = \boldsymbol{b},$$

where $\mathbf{N} \in \mathbb{R}^{m \times mn}$ and $\mathbf{M} \in \mathbb{R}^{n \times mn}$ are two matrices composed of "0" and "1". $\mathbf{N}$ and $\mathbf{M}$ in case of $m = n = 3$ are given, respectively, as

$$\mathbf{N} = \begin{pmatrix} 1 & 1 & 1 & 0 & 0 & 0 & 0 & 0 & 0 \\ 0 & 0 & 0 & 1 & 1 & 1 & 0 & 0 & 0 \\ 0 & 0 & 0 & 0 & 0 & 0 & 1 & 1 & 1 \end{pmatrix},$$

$$\mathbf{M} = \begin{pmatrix} 1 & 0 & 0 & 1 & 0 & 0 & 1 & 0 & 0 \\ 0 & 1 & 0 & 0 & 1 & 0 & 0 & 1 & 0 \\ 0 & 0 & 1 & 0 & 0 & 1 & 0 & 0 & 1 \end{pmatrix}.$$

Note that $\mathbf{N}$ and $\mathbf{M}$ both have a specific structure, where each column has only one single non-zero element and this is equal to 1.

Unbalanced Optimal Transport (UOT): The marginal constraints in (1) may exacerbate degradation of the performance of some applications where weights need not be strictly preserved. In contrast, the UOT problem *relaxes* them by replacing the equality constraints with penalty functions on the marginal distributions with a divergence. Formally, defining $\boldsymbol{y} = [\boldsymbol{a}, \boldsymbol{b}]^T$ and $\mathbf{X} = [\mathbf{M}^T, \mathbf{N}^T]^T$, the UOT problem can be formulated introducing a penalty function for the histograms as (Chapel et al., 2021)

$$\text{UOT}(\boldsymbol{a}, \boldsymbol{b}) := \min_{\boldsymbol{t} \in \mathbb{R}_+^{mn}} \boldsymbol{c}^T \boldsymbol{t} + D_\phi(\mathbf{X}\boldsymbol{t}, \boldsymbol{y}). \qquad (3)$$

It is worth mentioning that this function is convex due to the convexity of the Bregman divergence.

Relationship with Lasso-like problem: The Lasso-like problem has a general formula:

$$f(\boldsymbol{t}) \quad := \quad g(\boldsymbol{t}) + D_\phi(\mathbf{X}\boldsymbol{t}, \boldsymbol{y}).$$

Substituting $g(\boldsymbol{t}) = \lambda \|\boldsymbol{t}\|_1$ $(\lambda > 0)$ and $D_\phi(\mathbf{X}\boldsymbol{t}, \boldsymbol{y}) = \frac{1}{2}\|\mathbf{X}\boldsymbol{t} - \boldsymbol{y}\|_2^2$ into above reduces to the standard ℓ_2-norm regularized Lasso problem. On the other hand, addressing that $\boldsymbol{c}$ and $\boldsymbol{t}$ in (3) are nonnegative, the term $\boldsymbol{c}^T \boldsymbol{t}$ is represented as $\boldsymbol{c}^T \boldsymbol{t} = \sum_i c_i t_i = \sum_i c_i |t_i|$. Therefore, the UOT problem in (3) is equivalent to a weighted ℓ_1-norm regularized Lasso-like problem. It is, however, that $\mathbf{X} = [\mathbf{M}^T, \mathbf{N}^T]^T$ in (3) substantially differs from that of the Lasso problem. More concretely, the former $\mathbf{X}$ has a specific structure and has only two non-zero elements equal to 1 in each row whereas the latter $\mathbf{X}$ in Lasso problem is non-structured and dense (Chapel et al., 2021).

2.2   Dynamic Screening Framework

Solutions of many large-scale optimization problems tend to be sparse, and a large amount of computation is wasted on updating the zero elements during the optimization process. Screening technique is a well-known technique in the SVM (Ogawa et al., 2013) and Lasso problems, where the ℓ_1-norm regularizer leads to a sparse solution for the problem (Ghaoui et al., 2010). It can pre-select solutions that must be zero theoretically and freeze them before optimization computation, thus saving optimization time. Many safe screening methods have been proposed in this past decade (Liu et al., 2014; Wang et al., 2015), and recent dynamic screening methods efficiently drop variable elements, which include Dynamic Screening (Bonnefoy et al., 2015), Gap Safe screening (Ndiaye et al., 2017) and Dynamic Sasvi (Yamada and Yamada, 2021).

Hereinafter, we briefly elaborate on the framework proposed in (Yamada and Yamada, 2021) to introduce the whole dynamic screening technique for the Lasso-like problem:

$$\min_{\boldsymbol{t}} \{f(\boldsymbol{t}) := g(\boldsymbol{t}) + h(\mathbf{X}\boldsymbol{t})\}. \qquad (4)$$

The Fenchel-Rockafellar Duality yields the dual problem as presented below:

Theorem 1 (Fenchel-Rockafellar Duality (Rockafellar and Wets, 1998)). *If d and g are proper convex functions on $\mathbb{R}^{m+n}$ and $\mathbb{R}^{mn}$. Then we have the following:*

$$\min_{\boldsymbol{t}} g(\boldsymbol{t}) + h(\mathbf{X}\boldsymbol{t}) = \max_{\boldsymbol{\theta}} -h^*(-\boldsymbol{\theta}) - g^*(\mathbf{X}^T \boldsymbol{\theta}).$$

Because the primal function h is always convex, the dual function h^* is concave. Assuming h^* is an L-strongly concave problem, we can design an area for any feasible $\tilde{\boldsymbol{\theta}}$ by the strongly concave property:

Theorem 2 (L-strongly concave (Yamada and Yamada, 2021, Theorem 5)). *Considering problem in Eq.(4), if function d and g are both convex, for $\forall \tilde{\boldsymbol{\theta}} \in R^{m+n}$ and satisfied the constraints on the dual problem, we have the following area constructed by its L-strongly concave property:*

$$\mathcal{R}^C := \boldsymbol{\theta} \in \left\{ \frac{L}{2}\|\boldsymbol{\theta} - \tilde{\boldsymbol{\theta}}\|_2^2 + h^*(-\tilde{\boldsymbol{\theta}}) \le h^*(-\boldsymbol{\theta}) \right\}.$$

We know that the optimal solution for the dual problem $\hat{\boldsymbol{\theta}}$ satisfied the inequality, so the set is not empty.

3   PROPOSED UOT SCREENING

This section proposes a dynamic screening method designated to the UOT problem. For this purpose, we first derive the dual formulation of the Lasso-like formulated UOT problem in Eq.(3). Concrete proofs of lemma and theorems are provided in the supplementary file.

3.1 Dual formulation of UOT

As for the UOT problem in Eq.(3), function $h(\mathbf{X}t) = \frac{1}{2}\|\mathbf{X}t - \boldsymbol{y}\|_2^2$, and $g(\boldsymbol{\theta}) = \lambda \boldsymbol{c}^T t (\forall i, t_i > 0)$. We obtain the dual form by **Theorem 1**:

Lemma 3 (Dual form of UOT problem). *For UOT problem in Eq.(3), we obtain the following dual problem:*

$$-h^*(-\boldsymbol{\theta}) - g^*(\mathbf{X}^T\boldsymbol{\theta}) = -\frac{1}{2}\|\boldsymbol{\theta}\|_2^2 - \boldsymbol{y}^T\boldsymbol{\theta} \quad (5)$$
$$s.t. \qquad \boldsymbol{x}_p^T\boldsymbol{\theta} - \lambda c_p \leq 0, \forall p,$$

where $\boldsymbol{x}_p$ corresponds to the p-th column of $\mathbf{X}$.

It is clear that the strongly concave coefficient L for the dual function d is 1. These inequations in Eq.(5) make up a dual feasible area written as $\mathcal{R}^D$, and the optimal dual solution $\hat{\boldsymbol{\theta}} \in \mathcal{R}^D$ because of **??**.
The KKT condition of the UOT problem holds for the optimal primal and dual solutions $\hat{t}$ and $\hat{\boldsymbol{\theta}}$ that:

Theorem 4 (KKT condition). *For the dual optimal solution $\hat{\boldsymbol{\theta}}$, we have the following relationship:*

$$\boldsymbol{x}_p^T\hat{\boldsymbol{\theta}} - \lambda c_p \begin{cases} < 0 & \Rightarrow \hat{t}_p = 0 \\ = 0 & \Rightarrow \hat{t}_p \geq 0. \end{cases} \quad (6)$$

3.2 Detailed Screening Method

Eq.(6) indicates a potential method to screening the primal variable. Since we do not know the information of $\hat{t}$ directly, Screening techniques try to construct an area $\mathcal{R}^S$ as small as possible and also containing the $\hat{t}$, if

$$\max_{\boldsymbol{t} \in \mathcal{R}^S} \boldsymbol{x}_p^T\boldsymbol{\theta} - \lambda c_p < 0. \quad (7)$$

then we assert that:

$$\boldsymbol{x}_p^T\hat{\boldsymbol{\theta}} - \lambda c_p < 0, \quad (8)$$

which means the corresponding $\hat{t}_p = 0$, and can be screened out. Noteworthy point is that, for the UOT problem, $\boldsymbol{x}_p = [..., 0, 1, 0, ..., 0, 1, 0, ...,]^T$ has only two nonzero elements, p_1 and p_2, that are equal to 1. Therefore, we can set $\boldsymbol{\theta} = [\boldsymbol{u}^T, \boldsymbol{v}^T]^T$ and $\boldsymbol{u} \in \mathbb{R}^m, \boldsymbol{v} \in \mathbb{R}^n$, assuming $p = (I, J)$ where $I = p \mid m, J = p \mod m$. Subsequently, we rewrite Eq.(8) as

$$u_I + v_J - \lambda c_p < 0. \quad (9)$$

If we have $\tilde{\boldsymbol{\theta}} \in \mathcal{R}^D$, knowing from **Theorem ??**, we can construct the area $\mathcal{R}^C$ for the UOT problem:

Lemma 5 (The Circle Constraint for the UOT problem (Yamada and Yamada, 2021, Theorem 8)). *For the UOT problem in Eq.(3), $\mathcal{R}^C$ in **Theorem ??** is equal to a circle constraint:*

$$\mathcal{R}^C = \{\boldsymbol{\theta} \| (\boldsymbol{\theta} - \tilde{\boldsymbol{\theta}})^T(\boldsymbol{\theta} - \boldsymbol{y}) \leq 0\} \quad (10)$$

The $\boldsymbol{\theta}$ and $\boldsymbol{y}$ are the endpoints of the diameter of this circle. and $\hat{\boldsymbol{\theta}} \in \mathcal{R}^C$

If we obtain $\tilde{\boldsymbol{\theta}}$ in $\mathcal{R}^D$, combining $\mathcal{R}^D$ with $\mathcal{R}^C$ in **Lemma 5**, we can use $\mathcal{R}^C \cap \mathcal{R}^D$ as the area R^S in Eq.(8). However, maxmizing on the intersection of a hyper-ball and a polytope cannot be computed easily cause the $n+m$-polytope has nm Facets, (????) which costs too much for a screening operation.
The most direct method for dealing with the problem is to relax the polytope into a hyper-plane. Considering the specific structure of the $\mathbf{X}$ in the UOT problem, Our proposed method relaxes the polytope into two planes by combining the nm dual constraints with a positive weight $t_p \geq 0$, If the constraint is relevent to the dual elements I and j, which would influence the screening of t_p, we add it in group A, and the rest constraints are added in group B.

Theorem 6 (Two Plane Screening for UOT). *For every single primal variable t_p, let $A_p = \{i\|0 \leq i < nm, i \mid m = I \vee i \mod m = J\}$, and $B_p = \{i\|0 \leq i < nm, i \notin A_p\}$. Then, we construct a specific area $\mathcal{R}_p^S$ as presented below:*

$$\mathcal{R}_p^S = \left\{ \boldsymbol{\theta} \left\| \begin{array}{c} \sum_{l \in A_p} (\boldsymbol{\theta}^T \boldsymbol{x}_l t_l - \lambda c_l t_l) \leq 0, \\ \sum_{l \in B_p} (\boldsymbol{\theta}^T \boldsymbol{x}_l t_l - \lambda c_l t_l) \leq 0, \\ (\boldsymbol{\theta} - \tilde{\boldsymbol{\theta}})^T(\boldsymbol{\theta} - \boldsymbol{y}) \leq 0 \; (\textbf{Lemma5}) \end{array} \right. \right\}. \quad (11)$$

We have $\hat{t} \in \mathcal{R}^C \cap \mathcal{R}^D \subset \mathcal{R}_p^S$ (A simple proof process might be required for the $\subset$ relationship in the Appendix).

How does $\mathcal{R}_{IJ}^S$ play in the following??? Is in Algorithm 1 only?

We divide the constraints into two groups A_p and B_p for every single p, Our two-planes area $\mathcal{R}_{IJ}^S$ is smaller than the relaxation in (Yamada and Yamada, 2021). Benefiting from the structure of $\boldsymbol{x}_p$. As $\boldsymbol{x}_p^T\boldsymbol{\theta} = u_I + v_J$, these two dual elements are the optimization directions, and only $m+n$ constraints are directly connected with them, dividing the constraints in two groups by whether exists u_I, and v_J can alleviate the huge relaxation influence of other secondary dual variables. This problem can be solved easily by the Lagrangian method in constant time, the computational process is in Appendix. A
Before we start to screening with the area we constructed by **Lemma 5** and **Theorem 6**, we first have to find a dual variable $\tilde{\boldsymbol{\theta}} \in \mathcal{R}^D$. Although there exists a relationship between the primal variable and dual variable that $\boldsymbol{\theta} = \boldsymbol{y} - \mathbf{X}t$, inevitably, we often get

$\boldsymbol{\theta} \notin \mathcal{R}^D$. This requires us to project $\boldsymbol{\theta}$ onto $\mathcal{R}^D$. Dynamic Screening gets a more accurate screening outcome because the optimization algorithms gradually provide $\boldsymbol{t}^k \Rightarrow \hat{\boldsymbol{t}}$, and also the dual variable $\boldsymbol{\theta}^k \Rightarrow \hat{\boldsymbol{\theta}}$. If $\tilde{\boldsymbol{\theta}} \Rightarrow \hat{\boldsymbol{\theta}}$, the area $\mathcal{R}^C \cap \mathcal{R}^D$ would get smaller and has a better screening outcome. As the $\mathcal{R}^D$ is a polytope combined with nm hyperplanes, the real projection is solved no matter by Linear programming or Dykstra's projection algorithm cost too much. In the Standard Lasso problem, the dual constraints in Eq.(5) is $\|\boldsymbol{x}_p \hat{\boldsymbol{\theta}}\|_1 \leq \lambda$, x_p is almost dense and irregular, one use a simple shrinking method to obtain a $\tilde{\boldsymbol{\theta}} \in \mathcal{R}^D$: **?**:

$$\tilde{\boldsymbol{\theta}} = \frac{\boldsymbol{\theta}}{\max(1, \|\frac{\mathbf{X}^T \boldsymbol{\theta}}{\lambda}\|_\infty)}$$

The Standard Lasso projection pushes the $\boldsymbol{\theta}$ far away from the optimum $\hat{\boldsymbol{\theta}}$, it suffers from the influence of small $\boldsymbol{c}_p$ in the UOT problem as

$$\tilde{\boldsymbol{\theta}} = \frac{\boldsymbol{\theta}}{\max(1, \|\frac{\mathbf{X}^T \boldsymbol{\theta}}{\lambda \boldsymbol{c}^T}\|_\infty)}$$

It will degenerate when one of the costs is $c_p = 0$, and disable the screening process. Therefore, noting that, for the UOT problem, it only allows $t_p \geq 0$, and the $\boldsymbol{x}_p$ only consists of two non-zero elements, we can adapt a better and cheap projection method. The following theorem states this:

Theorem 7 (UOT shifting projection). *For any* $\boldsymbol{\theta} = [\boldsymbol{u}^T, \boldsymbol{v}^T]^T$, *we compute the projection* $\tilde{\boldsymbol{\theta}} = [\tilde{\boldsymbol{u}}^T, \tilde{\boldsymbol{v}}^T]^T \in \mathcal{R}^D$ *as*

$$\begin{aligned}
\tilde{u}_I &= u_I - \max_{0 \leq j < n} \frac{u_I + v_j - \lambda c_p}{2} \\
&= \frac{u_I + \lambda c_p}{2} - \frac{1}{2} \max_{0 \leq j < n} v_j \qquad (12) \\
\tilde{v}_J &= v_J - \max_{0 \leq i < m} \frac{u_i + v_J - \lambda c_p}{2} \\
&= \frac{v_J + \lambda c_p}{2} - \frac{1}{2} \max_{0 \leq i < m} u_j \qquad (13)
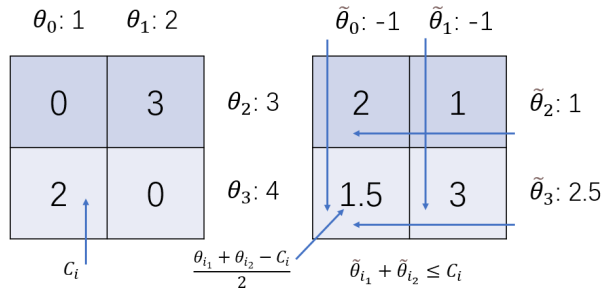\end{aligned}$$

Figure 1: Shifting on a 2×2 matrix

We shift every single u_I, v_J with half of the maximum differences in all of its constraints, this cheap projection method can get good accuracy with $O(nm)$ computational time. The proof process is in the Appendix
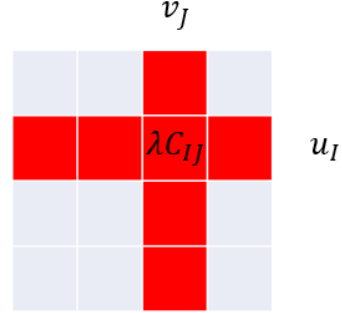

Figure 2: Selection of group A_{IJ}(red) and B_{IJ}(grey)

3.3 Screening Algorithms

Algorithm 1 UOT Dynamic Screening Algorithm

Input: $\boldsymbol{t}_0, \boldsymbol{s} \in R^{nm}, s_p = 1$
Output: $\boldsymbol{s}$
    Choose a solver for the problem.
    for $k = 0$ to $K - 1$ **do**
        Projection $\tilde{\boldsymbol{\theta}}^k = \text{Proj}(\boldsymbol{t}^k)$ **Theorem7**
        for $p = 0$ to $mn - 1$ **do**
            $\mathcal{R}^S \leftarrow \mathcal{R}_p^S(\tilde{\boldsymbol{\theta}}^k, \boldsymbol{t}^k)$
            $\boldsymbol{s} \leftarrow s_p = 0$ if $\max_{\boldsymbol{\theta} \in \mathcal{R}^S} \boldsymbol{x}_p^T \boldsymbol{\theta}^k < \lambda c_p$ **Theorem 6**
        end for
        for $p \in \{p \| s_p = 0\}$ **do**
            $\boldsymbol{t}_p^k \leftarrow 0$
        end for
        $\boldsymbol{t}^{k+1} = \text{update}(\boldsymbol{t}^k)$
    end for
    return $\boldsymbol{t}^{K+1}, \boldsymbol{s}$

(Insert equation numbers in appropriate lines in **Algorithm ??**

It should be emphasized that the proposed screening method is *independent* of the optimization solver that you choose. We give the specific algorithm for L_2 UOT problem to show the whole optimization process as in **Algorithm 1**. The update($\boldsymbol{t}$) operator in the algorithm indicates the updating process for $\boldsymbol{t}$ according to the adopted optimizer. $\boldsymbol{s}$ is the screening mask vector for the transport vector $\boldsymbol{t}$, when $s_p = 0$, it means the t_p should be screened out.

3.4 Computational Cost Analysis

XXXXXX

4 EXPERIMENTS

In this section, we show the efficacy of the proposed methods using toy Gaussian models and the MNIST dataset.

4.1 Projection Method

To prove the effectiveness of our projection method compared with the traditional projection method in the Lasso problem, we compared the projection distance and screening ratio with randomly generated Gaussian measures by two projection methods. We set the $\lambda = \frac{\|\mathbf{X}^T y\|}{100}$ and test for 10 different pairs. We choose the FISTA for solving the L_2 penalized UOT problems. Our projection method has only moved the dual point by a very small order of magnitude. It ensures that the points are kept at a smaller distance from the optimal solution and cause better screening effects.
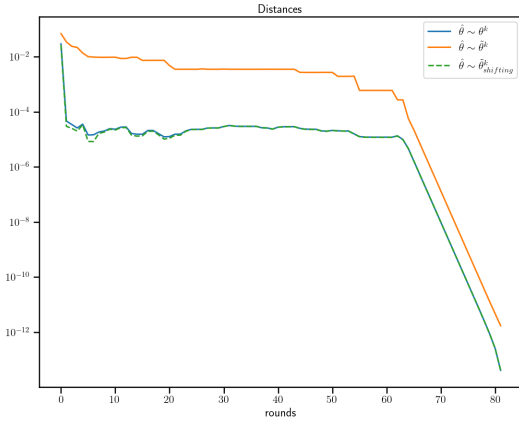
Figure 3: Distance of different projection method

4.2 Divide Method

We compared the screening ratio with three different methods, including our Divide method, Dynamic Sasvi method, and Gap method. Every method would use our projection method to get a better outcome, which also makes sure the difference in performance is only in the construction of the feasible domain.
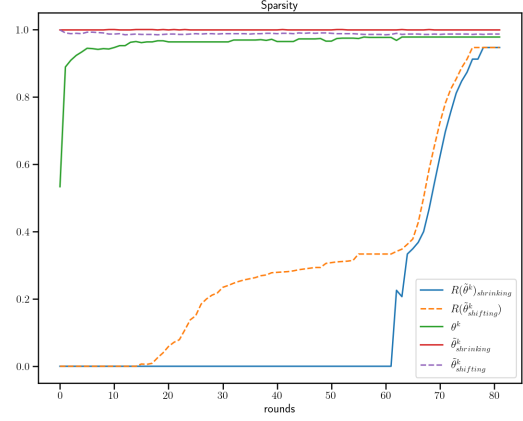
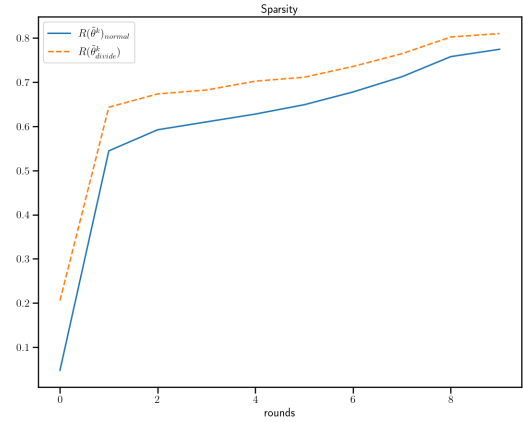

Figure 4: Screening ratio of different projection method

Figure 5: Screening ratio of dividing method

4.3 Best Divide Method

We compared the screening ratio with three different methods, including our Divide method, the Dynamic Sasvi method, and a random divide method.

4.4 Speed up Ratio

We choose the FISTA method, Newton method, and Language method to test the screening ratio.

5 CONCLUSION

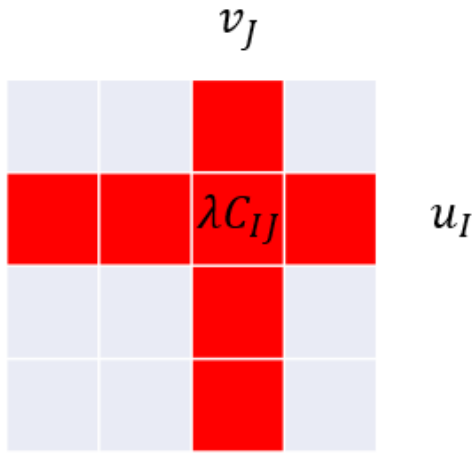Our algorithm is great, we are going to apply the method onto Sinkhorn

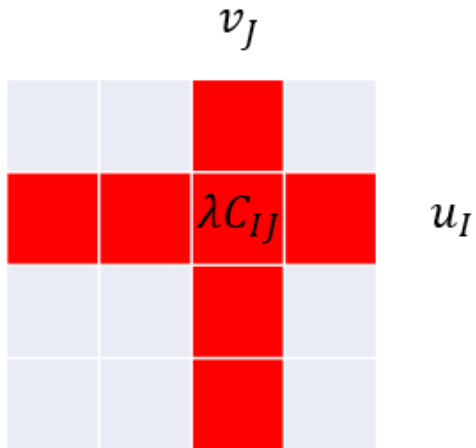Figure 6: Comparing of our separation method with random separation method

Figure 7: speed up ratio for different solver

References

Arjovsky, M., Chintala, S., and Bottou, L. (2017). Wasserstein generative adversarial networks. In *International conference on machine learning*, pages 214–223. PMLR.

Benamou, Jean-David (2003). Numerical resolution of an "unbalanced" mass transport problem. *ESAIM: M2AN*, 37(5):851–868.

Blondel, M., Seguy, V., and Rolet, A. (2018). Smooth and sparse optimal transport. In *AISTATS*.

Bonnefoy, A., Emiya, V., Ralaivola, L., and Gribonval, R. (2015). Dynamic screening: Accelerating first-order algorithms for the lasso and group-lasso. *IEEE Transactions on Signal Processing*, 63(19):5121–5132.

Caffarelli, L. A. and McCann, R. J. (2010). Free boundaries in optimal transport and Monge-Ampère obstacle problems. *Annals of Mathematics*, 171(2):673–730.

Chapel, L., Flamary, R., Wu, H., Févotte, C., and Gasso, G. (2021). Unbalanced optimal transport through non-negative penalized linear regression. In *NeurIPS*.

Chen, L., Zhang, Y., Zhang, R., Tao, C., Gan, Z., Zhang, H., Li, B., Shen, D., Chen, C., and Carin, L. (2019). Improving sequence-to-sequence learning via optimal transport. In *7th International Conference on Learning Representations, ICLR 2019*. International Conference on Learning Representations, ICLR. Generated from Scopus record by KAUST IRTS on 2021-02-09.

Chizat, L., Peyré, G., Schmitzer, B., and Vialard, F.-X. (2017). Scaling algorithms for unbalanced transport problems. *arXiv preprint: arXiv:1607.05816*.

Courty, N. (2017). Optimal transport for domain adaptation. *IEEE Transactions on Pattern Analysis and Machine Intelligence*, 39(9):1853–1865.

Cuturi, M. (2013). Sinkhorn distances: Lightspeed computation of optimal transport. In Burges, C., Bottou, L., Welling, M., Ghahramani, Z., and Weinberger, K., editors, *Advances in Neural Information Processing Systems*, volume 26. Curran Associates, Inc.

Efron, B., Hastie, T., Johnstone, I., and Tibshirani, R. (2004). Least angle regression. *Annals of Statistics*, 32:407–489.

Ghaoui, L. E., Viallon, V., and Rabbani, T. (2010). Safe feature elimination for the lasso and sparse supervised learning problems. *arXiv preprint arXiv:1009.4219*.

Janati, H., Cuturi, M., and Gramfort, A. (2019). Wasserstein regularization for sparse multi-task regression. In *AISTATS*.

Kantorovich, L. (1942). On the transfer of masses. *Dokl. Akad. Nauk*, 37(2):227–229.

Lee, D. D. and Seung, H. S. (2000). Algorithms for non-negative matrix factorization. In *NIPS*.

Liero, M., Mielke, A., and Savaré, G. (2018). Optimal entropy-transport problems and a new hellinger–kantorovich distance between positive measures. *Inventiones mathematicae*, 211(3):969–1117.

Liu, J., Zhao, Z., Wang, J., and Ye, J. (2014). Safe screening with variational inequalities and its application to lasso. In *ICML*.

Maretic, H. P., Gheche, M. E., Chierchia, G., and Frossard, P. (2019). GOT: An optimal transport framework for graph comparison. In *NeurIPS*.

Ndiaye, E., Fercoq, O., Alex, re Gramfort, and Salmon, J. (2017). Gap safe screening rules for sparsity enforcing penalties. *Journal of Machine Learning Research*, 18(128):1–33.

Nguyen, Q. M., Nguyen, H. H., Zhou, Y., and Nguyen, L. M. (2022). On unbalanced optimal transport: Gradient methods, sparsity and approximation error. *arXiv preprint arXiv:2202.03618*.

Ogawa, K., Suzuki, Y., and Takeuchi, I. (2013). Safe screening of non-support vectors in pathwise SVM computation. In *ICML*.

Pham, K., Le, K., Ho, N., Pham, T., and Bui, H. (2020). On unbalanced optimal transport: An analysis of Sinkhorn algorithm. In *ICML*.

Rockafellar, R. T. and Wets, R. J. B. (1998). *Variational Analysis*. Springer.

Schiebinger, G., Shu, J., Tabaka, M., Cleary, B., Subramanian, V., Solomon, A., Gould, J., Liu, S., Lin, S., Berube, P., Lee, L., Chen, J., Brumbaugh, J., Rigollet, P., Hochedlinger, K., Jaenisch, R., Regev, A., and Lander, E. S. (2019). Optimal-transport analysis of single-cell gene expression identifies developmental trajectories in reprogramming. *Cell*, 176(4):928–943.e22.

Schmitzer, B. (2016). Stabilized sparse scaling algorithms for entropy regularized transport problems. *CoRR*, abs/1610.06519.

Sinkhorn, R. (1974). Diagonal equivalence to matrices with prescribed row and column sums. ii. *Proceedings of the American Mathematical Society*, 45(2):195–198.

Tibshirani, R. (1996). Regression shrinkage and selection via the lasso. *Journal of the Royal Statistical Society. Series B (Methodological)*, 58(1):267–288.

Villani, C. (2008). *Optimal Transport: Old And New.* Springer.

Wang, J., Wonka, P., and Ye, J. (2015). Lasso screening rules via dual polytope projection. *Journal of Machine Learning Research*, 16:1063–1101.

Yamada, H. and Yamada, M. (2021). Dynamic sasvi: Strong safe screening for norm-regularized least squares. In Ranzato, M., Beygelzimer, A., Dauphin, Y., Liang, P., and Vaughan, J. W., editors, *Advances in Neural Information Processing Systems*, volume 34, pages 14645–14655. Curran Associates, Inc.

Yang, K. D. and Uhler, C. (2019). Scalable unbalanced optimal transport using generative adversarial networks. In *ICLR*.

Supplementary Material: Dynamic Screening for ℓ_2-norm Penalized Unbalanced Optimal Transport Problem

A PROOFS

A.1 Proof of Theorem 7

For any $p \in 0, 1, ..., nm - 1$ we assume that $p = (I, J)$, then we can compute that:

$$
\begin{aligned}
\boldsymbol{x}_p^T \tilde{\boldsymbol{\theta}} &= \tilde{\boldsymbol{u}}_I + \tilde{\boldsymbol{v}}_J \\
&= \boldsymbol{u}_I + \boldsymbol{v}_J - \max_{0 \geq j \geq n} \frac{\boldsymbol{u}_I + \boldsymbol{v}_j - \lambda \boldsymbol{c}_p}{2} - \max_{0 \geq i \geq m} \frac{\boldsymbol{u}_i + \boldsymbol{v}_J - \lambda \boldsymbol{c}_p}{2} \\
&= \frac{\boldsymbol{u}_I + \boldsymbol{v}_J}{2} - \max_{0 \geq j \geq n} \frac{\boldsymbol{v}_j}{2} - \max_{0 \geq i \geq m} \frac{\boldsymbol{u}_i}{2} + \lambda \boldsymbol{c}_p \\
&= \frac{1}{2} \boldsymbol{x}_p^T \boldsymbol{\theta} - \max_{0 \geq j \geq n} \frac{\boldsymbol{v}_j}{2} - \max_{0 \geq i \geq m} \frac{\boldsymbol{u}_i}{2} + \lambda \boldsymbol{c}_p \\
&\leq \lambda \boldsymbol{c}_p
\end{aligned}
\tag{14}
$$

For $\forall p$, we have $\tilde{\boldsymbol{\theta}} \in \mathcal{R}^D$

A.2 Proof of Theorem 6

We Generalize the problem as

$$
\max_{\boldsymbol{\theta} \in \mathcal{R}_I^S} \boldsymbol{\theta}_{I_1} + \boldsymbol{\theta}_{I_2}
\tag{15}
$$

Considering the center of the circle as $\boldsymbol{\theta}^o$, we define $\boldsymbol{\theta} = \boldsymbol{\theta}^o + q$, as $\boldsymbol{\theta}_{I_1}^o + \boldsymbol{\theta}_{I_2}^o$ is a constant, the problem is equal to $\min_{\boldsymbol{\theta} \in \mathcal{R}_I^S} -(\boldsymbol{q}_{I_1} + \boldsymbol{q}_{I_2})$, we compute the Lagrangrian function of later:

$$
\min_{\boldsymbol{q}} \max_{\eta, \mu, \nu \geq 0} L(\boldsymbol{q}, \eta, \mu, \nu) = \min_{\boldsymbol{q}} \max_{\eta, \mu, \nu \geq 0} -\boldsymbol{q}_{I_1} - \boldsymbol{q}_{I_2} + \eta(\boldsymbol{q}^T \boldsymbol{q} - r^2) + \mu(a^T \boldsymbol{q} - e_a) + \nu(b^T \boldsymbol{q} - e_b)
\tag{16}
$$

$$
\frac{\partial L}{\partial \boldsymbol{q}_i} =
\begin{cases}
-1 + 2\eta \boldsymbol{q}_i + \mu a_i + \nu b_i & i = I_1, I_2 \\
2\eta \boldsymbol{q}_i + \mu a_i + \nu b_i & i \neq I_1, I_2
\end{cases}
\tag{17}
$$

$$
\boldsymbol{q}_i^* =
\begin{cases}
\dfrac{1 - \mu a_i - \nu b_i}{2\eta} & i = I_1, I_2 \\[2mm]
-\dfrac{\mu a_i + \nu b_i}{2\eta} & i \neq I_1, I_2
\end{cases}
\tag{18}
$$

We can get the Lagrangian dual problem:

$$
\max_{\eta, \mu, \nu \geq 0} L(\eta, \mu, \nu) = \max_{\eta, \mu, \nu \geq 0} \frac{\mu a_{I_1} + \nu b_{I_1} - 1}{2\eta} + \frac{\mu a_{I_2} + \nu b_{I_2} - 1}{2\eta} + \eta(\boldsymbol{q}^{*T} \boldsymbol{q}^* - r^2) + \mu(a^T \boldsymbol{q}^* - e_a) + \nu(b^T \boldsymbol{q}^* - e_b)
\tag{19}
$$

From the KKT optimum condition, we know that if

$$
\begin{aligned}
\eta(\boldsymbol{q}^{*T} \boldsymbol{q}^* - r^2) &= 0 \\
\mu(a^T \boldsymbol{q}^* - e_a) &= 0 \\
\nu(b^T \boldsymbol{q}^* - e_b) &= 0
\end{aligned}
\tag{20}
$$

We set η^*, μ^*, ν^* as the solution of the equations, which is also the solution of the dual problem. Firstly, we assume that $\eta^*, \mu^*, \nu^* \neq 0$, then the solution is equal to compute the following equations:

$$(1 - \mu a_{I_1} - \nu b_{I_1})^2 + (1 - \mu a_{I_2} - \nu b_{I_2})^2 + \sum_{i \neq I_1, I_2}^{m+n} (a_i \mu + b_i \nu)^2 - 4\eta^2 r^2 = 0$$

$$a_{I_1} - \mu a_{I_1}^2 - \nu b_{I_1} a_{I_1} + a_{I_2} - \mu a_{I_2}^2 - \nu b_{I_2} a_{I_2} - \sum_{i \neq I_1, I_2}^{m} (a_i^2 \mu + b_i a_i \nu) - 2\eta e_a = 0 \quad (21)$$

$$b_{I_1} - \nu b_{I_1}^2 - \mu b_{I_1} a_{I_1} + b_{I_2} - \nu b_{I_2}^2 - \mu b_{I_2} a_{I_2} - \sum_{i \neq I_1, I_2}^{m} (b_i^2 \nu + b_i a_i \mu) - 2\eta e_b = 0$$

Rearranged as:

$$2 - 2\mu(a_{I_1} + a_{I_2}) - 2\nu(b_{I_1} + b_{I_2}) + \|a\|^2 \mu^2 + \|b\|^2 \nu^2 + 2\mu\nu a^T b - 4\eta^2 r^2 = 0$$
$$(a_{I_1} + a_{I_1}) - \|a\|^2 \mu - a^T b \nu - 2\eta e_a = 0 \quad (22)$$
$$(b_{I_1} + b_{I_2}) - \|b\|^2 \nu - a^T b \mu - 2\eta e_b = 0$$

we have

$$\mu = \frac{2(e_b a^T b - e_a \|b\|^2)\eta + (a_{I_1} + a_{I_2})\|b\|^2 - (b_{I_1} + b_{I_2})(a^T b)}{\|a\|^2 \|b\|^2 - a^T b}$$

$$\nu = \frac{2(e_a a^T b - e_b \|a\|^2)\eta + (b_{I_1} + b_{I_2})\|a\|^2 - (a_{I_1} + a_{I_2})(a^T b)}{\|a\|^2 \|b\|^2 - a^T b} \quad (23)$$

set it as:

$$\mu = s_1 \eta + s_2$$
$$\nu = u_1 \eta + u_2 \quad (24)$$

Then we can solve the η as a quadratic equation:

$$0 = a\eta^2 + b\eta + c$$
$$a = 4r^2 - s_1^2 \|a\|^2 - u_1^2 \|b\|^2 - 2s_1 u_1 a^T b$$
$$b = 2(a_{I_1} + a_{I_2})s_1 + 2(b_{I_1} + b_{I_2})u_1 - 2s_1 s_2 \|a\|^2 - 2u_1 u_2 \|b\|^2 - 2(s_1 u_2 + s_2 u_1)a^T b \quad (25)$$
$$c = 2(a_{I_1} + a_{I_2})s_2 + 2(b_{I_1} + b_{I_2})u_2 - s_2^2 \|a\|_1 - u_2^2 \|b\|_1 - 2s_2 u_2 a^T b - 2$$

Then we can put it back into 24 and get μ, ν.

If the solution satisfied the constraints $\eta^*, \mu^*, \nu^* > 0$, then it is the solution. However, if one of the dual variables is less than 0, the problem would degenerate into a simpler question.

If only η^* is larger than 0, $\min_{\boldsymbol{\theta} \in \mathcal{R}_I^S} -(\boldsymbol{q}_{I_1} + \boldsymbol{q}_{I_2}) = -\sqrt{2}r$

If only μ^* or ν^* is less than 0, we are optimizing on a sphere cap, the solution can be found in (Yamada and Yamada, 2021, Appendix B)

if only $\eta^* \leq 0$: As the sphere is inactivated, the problem gets maximum at every point of the intersection of two planes.

$$\min_{\boldsymbol{q}} \max_{\mu,\nu \geq 0} L(\boldsymbol{q}, \mu, \nu) = \min_{\boldsymbol{q}} \max_{\mu,\nu \geq 0} -\boldsymbol{q}_{I_1} - \boldsymbol{q}_{I_2} + \mu(a^T \boldsymbol{q} - e_a) + \nu(b^T \boldsymbol{q} - e_b) \quad (26)$$

To have a solution, the equations satisfied

$$\frac{\partial L}{\partial q} = \begin{cases} -1 + \mu a_i + \nu b_i = 0 & i = I_1, I_2 \\ -\mu a_i - \nu b_i = 0 & i \neq I_1, I_2 \end{cases} \quad (27)$$

As the equation satisfied, we can just set $\boldsymbol{q}_i^* = 0, i \neq I_1, I_2$, then we compute the

$$\min_{\boldsymbol{\theta} \in \mathcal{R}_I^S} -(\boldsymbol{q}_{I_1} + \boldsymbol{q}_{I_2}) = \frac{a_{I_2}e_b - b_{I_2}e_a - a_{I_1}e_b + b_{I_1}e_a}{a_{I_1}b_{I_2} - a_{I_2}b_{I_1}} \tag{28}$$